ANALYSIS OF RESIDUAL STRESSES AND DURABILITY OF THE CUTTING INSERTS AFTER DIAMOND-SPARK GRINDING

Yury Sizyi, *Prof. Dr Eng., sizy.iury@yandex.ua,*
Nat. Tech. Univ. "Kharkov Polytech. Inst.", Kharkov, Ukraine
Roman Strelchuk, *ME Doctoral Candidate, r.m.strelchuk@gmail.com,*
Nat. Tech. Univ. "Kharkov Polytech. Inst.", Kharkov, Ukraine
Shailendra Kumar Jha, *Prof. Dr Eng., skjha63@rediffmail.com,*
University of Delhi, New Delhi, India
Alexander Rudnev, *Sen. Staff Scientist, grinko@kpi.kharkov.ua,*
Nat. Tech. Univ. "Kharkov Polytech. Inst.", Kharkov, Ukraine
Yury Gutsalenko, *Sen. Staff Scientist, gutsalenko@kpi.kharkov.ua,*
Nat. Tech. Univ. "Kharkov Polytech. Inst.", Kharkov, Ukraine

Abstract: The article presents an analysis of residual stresses and resistance of cutting inserts after the diamond-spark grinding. In the entire investigated range of traverses (0.01...0.07mm/double stroke) and wheel speed (18...32m/s), the total residual oriented stresses in both phases are compressive and they have an extreme character with a point of extremum (minimum) in the center of the interval ($S_{поп}$ = 0.04mm/double stroke; $V_{кр}$ = 25m/s). In the carbide phase, the main share in the formation of the total stress state of the surface layer of the STIM-3B (СТИМ-3Б) hard alloy is made by macrostresses. The mechanism of their formation is thermal at small and large values of the traverse and wheel speed, and power one—at medium values. The importance of interfacial microstresses in this phase is minor. In the binding phase of nickel, the interfacial component contributes significantly to the formation of the general stress state, due to the force factor at average values of the grinding mode mechanical parameters and thermal parameters in the rest of the range. The highest wear resistance of tools made of STIM-3B (СТИМ-3Б) alloy corresponds to the highest value of compressive interfacial microstresses in the plastic phase (Ni).
Keywords: residual stresses, grinding wheel, carbide, tool durability.

Introduction

The possibility of dividing the total oriented stresses into macrostresses and interfacial microstresses allows a differentiated approach to the analysis of the relationship of the durability of a tool made of STIM-3B (СТИМ-3Б) alloy with each component of stress and general total stresses.

Therefore, to determine the area of optimal modes of diamond-spark grinding, taking into account the operational properties, the possibility of establishing a relationship between the machining conditions, the stress state of the surface layer, and the durability of the cutters in real operating conditions has been studied; life testings have been carried out for tools processed in the appropriate conditions of the diamond-spark grinding.

Research Methodology

Residual oriented stresses in the surface layer of STIM-3B (СТИМ-3Б) heterogeneous hard alloy have been determined by X-ray multiple oblique surveys ($\sin^2\psi$ – method) [1, 2]. The interplanar spacings have been measured on a Dron-3 ("Дрон-3") diffractometer in copper radiation. The deformation of the crystal lattice of the ground samples of STIM-3B (СТИМ-3Б) alloy has been measured by the shift of lines (511) for the TiC phase and (331) for the Ni phase. Oblique surveys have been carried out at angles of 0°; ±20°; ±40°; ±50°.

The value of residual stresses has been found by the formula:

$$\sigma = \frac{E}{1+\mu} \cdot \frac{d_{\psi} - d_{\perp}}{d \perp} \cdot \frac{1}{\sin^2 \psi}, \quad (1)$$

where E – modulus of elongation; μ – Poisson's ratio; d_{ψ}, $d_{\perp}$ – interplanar spacings measured at an angle and normal to the sample surface; ψ – the angle between the normal to the sample surface and the corresponding normal to the reflecting planes.

Macroscopic values of the moduli of elongation and Poisson's ratios are taken for stress calculations: for titanium carbide (TiC) – E = 460GPa; μ = 0.17; for nickel (Ni) – E = 210GPa; μ = 0.30.

Experiments to determine the tool durability of STIM-3B (СТИМ-3Б) hard alloy have been carried out on a 16K20 screw-cutting lathe when turning 45 (HB 190) untempered steel without cooling under the following modes: V = 3.25m/s; S = 0.075mm/r; t = 0.2mm. The cutters had the following geometric parameters: γ = 0°; α = 12°; φ = 45°; φ_1 = 15°; λ = 0. The bluntness criterion was taken as the flank wear h_3 = 0.45mm, which was measured directly on the lathe using a Mir-2 (Мир-2) microscope.

Results

Fig. 1 and Fig 2 show the test results of cutters made of STIM-3B (СТИМ-3Б) alloy; they provide the tool durability vs. traverse and grinding speed.

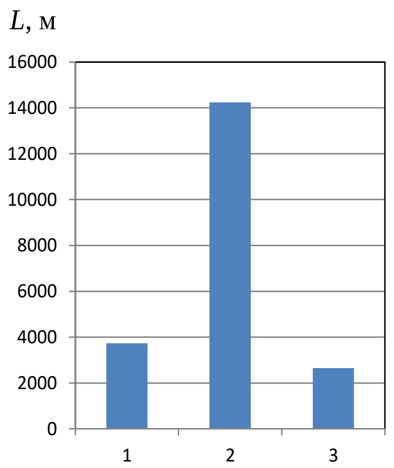

Fig. 1. Cutting path length from the traverse grinding: 1. $S_{поп}$=0.01mm/double stroke, 2. $S_{поп}$=0.04mm/double stroke, 3. $S_{поп}$=0.07mm/double stroke

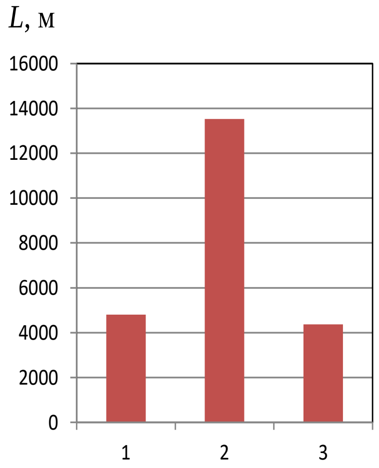

Fig. 2. Cutting path length vs. grinding speed: 1. V =18m/s, 2. V =25m/s, 3. V =32m/s

Before analyzing the relationship of residual stresses and the length of the cutting path to a given wear criterion, it is advisable to consider the change in stresses for different grinding modes of inserts and the contribution of individual components (macro- and interfacial microstresses) to the general stress state (total stresses).

With an increase in the traverse from 0.01mm/double stroke to 0.07mm/double stroke in the carbide phase (TiC), residual stresses (Fig. 3a) appear, varying from 390MPa to 270MPa. In the cementing phase (Ni), a non-monotonic dependence of the total compressive stresses on the traverse is also observed from 230MPa to 130MPa at the central point and up to 250MPa (Fig. 3b).

With an increase in the wheel speed from 18m/s to 32m/s, the non-monotonic nature of the change in the total compression stresses remains: in the carbide phase (TiC), they change from 460MPa to 280MPa, and in the cementing phase (Ni)—from 220MPa to 190MPa.

A joint analysis of the dependencies of the change in the length of the cutting path (Fig. 1, 2) and total stresses (Fig. 3) on the traverse shows that the lowest (in absolute value) total compressive stresses correspond to the greatest durability. A similar relationship can be traced in the work [3] when machining TN20 alloys.

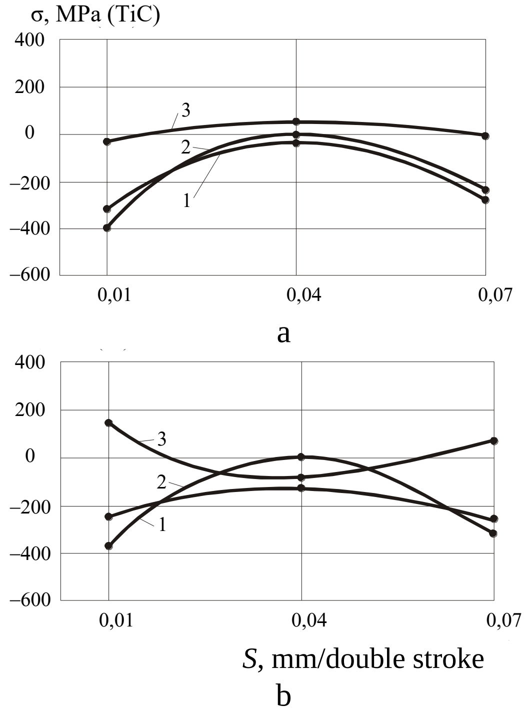

Fig. 3. Influence of traverse on residual stresses in TiC and Ni phases.
1 – total oriented stresses
2 – macrostresses
3 – interfacial microstresses
Grinding conditions:
V = 25m/s; $S_{прод}$ = 1.5m/min

Further, it is advisable to consider the relationship of durability with the individual components of the total compressive stresses—interfacial microstresses in each of the phases and the macrocomponent.

In STIM-3B (СТИМ-3Б) tungstenless hard alloy owing to the heterogeneous structure, interfacial microstresses of thermal and force origin interact due to the internal inhomogeneity of the thermophysical properties of the phases, as well as macrostresses due to external inhomogeneous plastic and thermoplastic deformation during machining. The research results show that at all machining modes, the formation of macrostresses (σ_1) occurs, according to the force mechanism, as evidenced by their compressive nature (Fig. 3). It should be noted that in TN 20 (TH 20) tungstenless hard alloy, the formation of a macrostressed state also occurs with the prevalence of the force factor.

As for the mechanism of the formation of interfacial microstresses, it is different in the carbide and cementing phases and depends on the machining mode. So, in the TiC phase, with a change in the traverse from 10mm/double stroke to 0.07mm/double stroke, an extreme dependence is revealed, microstresses pass from compressive (-10MPa) to tensile (+10MPa) and then—to zero level (Fig. 3); it can be noted that the thermal and force mechanisms make approximately the same contribution to the formation of interfacial microstresses in this phase. Analysis of interfacial microstresses in the carbide phase shows that their share in the general total stresses is very insignificant.

In the cementing phase, this contribution is already significant. So, with $S_{поп}$ = 0.04mm/double stroke and $V_{кр}$ = 25m/s, the absolute value of microstresses is about 1,000% of the magnitude of macrostresses. When the traverse is changed from 0.01mm/double stroke to 0.07mm/double stroke, an extreme dependence of the interfacial microstresses on the traverse value takes place. In this case, their value changes, passing from tensile stresses (+150MPa) to compressive (-120MPa) and again to tensile ones (+20MPa). With an increase in the wheel speed from 18m/s to 32m/s in the cementing phase, an extreme dependence is also manifested, the value of interfacial microstresses goes from tensile stresses (+230MPa) into compressive (-120MPa) and then again into tensile ones (+90MPa) (Fig. 3).

The magnitude of the interfacial microstresses in the carbide phase (TiC) is very insignificant for all the considered values of the wheel speed, which indicates their weak role in comparison with macrostresses. As with a change in the traverse, the macrostresses are compressive and practically coincide with the total oriented stresses. Their value varies from (-450MPa) to (-280MPa).

Thus, based on the studies, the following assumptions can be made: in the carbide phase, the main share in the formation of the stressed surface layer of STIM-3B (СТИМ-3Б) hard alloy is made by macrostresses, the mechanism of their formation is of a force nature, and the contribution of interfacial microstresses in this phase is small.

In the cementing phase, the interfacial microcomponent contributes to the formation of the general stress state of the surface layer. In this case, the force mechanism of stress formation is of predominant importance. The share of the thermal factor is small here. Comparing the results of life testings (Fig. 1 and Fig. 2) with the dependences of the total residual stresses, macro- and microstresses in different phases on the traverse and wheel speed, it is possible to identify the relationship between tool durability from STIM-3B (СТИМ-3Б) alloy and the corresponding residual stresses.

The highest absolute compressive interfacial microstresses in the plastic phase (Ni) correspond to the highest durability of cutting inserts. It is known that the relationship between the tool wear resistance and the residual voltage level in some works is characterized by a relationship, in which large total compressive stresses correspond to the large durability of the cutting tool [4, 5]. Meanwhile, this dependence is not confirmed for STIM-3B (СТИМ-3Б) alloys under study. Let's consider the possible reasons for the different effect of oriented residual stresses in STIM-3B (СТИМ-3Б) alloy on the wear resistance of cutters.

The analysis has shown that the difference in the composition, microstructure, physicomechanical and thermophysical properties of alloys is manifested in the depth of propagation of macrostresses, as well as in the specific features of the formation of interfacial microstrain (microstresses) [6, 7].

In STIM-3B (СТИМ-3Б) alloys, the depth of propagation of the macrostressed state in the carbide phase, investigated by layer-by-layer X-ray diffraction, is insignificant and reaches about 15–20μm.

As for the contribution of interfacial microstrain to the general stress state of the STIM (СТИМ) alloy, the mechanism of formation and the fraction of the microcomponent of permanent deformation significantly depends on the machining mode; interfacial microstrain makes a significant contribution to the resulting stress state, which exceeds the fraction of macrostrain in the grinding mode, which provides maximum durability of cutting inserts.

This fact, as well as the shallow depth of the macrostressed zone, indicates that in STIM-3B (СТИМ-3Б) alloys, the oriented lattice deformation measured in two phases reflects to a greater extent the behavior of the interfacial microscopic stress state, rather than the macroscopic component.

It can be assumed that, under conditions of fine turning of steel, an external tensile load occurs in the surface layer of the STIM-3B (СТИМ-3Б) alloy, and therefore, the crystallites of the phase with tensile interfacial microstrain, that is, cementing, are likely to be the "weak" link. In this case, the resulting stress state is determined by the superposition of residual stresses and the load (stresses) from the external force [8, 9]. This, obviously, can explain that higher values of tensile interfacial microstresses in the cementing phase correspond to lower wear resistance of the cutters.

Conclusions

Thus, the type and conditions of the contact interaction of tools during their operation largely determine the nature of their wear. When turning at high heating temperatures, which is especially characteristic of tungstenless hard alloys with low thermal conductivity, the wear mechanism can be affected by shear displacements of atoms, for example, as a result of diffusion; as is known, zones with microstresses and lattice distortions are more susceptible to diffusion.

Carbon diffusion can cause nonstoichiometry of TiC, an increase in carbon deficiency, and, as a consequence, a decrease in the strength and microhardness of titanium carbide. Moreover, interfacial microstresses can promote oxidation of TiC even at 500–600°C.

Interfacial microstresses, finally, can promote the diffusion of iron into a hard alloy, partially replacing nickel and leading to a weakening of carbides in STIM-3B (СТИМ-3Б) alloy. Consequently, in each case, depending on the composition of the material, its properties, grinding conditions, and the operation of tools, any of the phases of the heterogeneous material, in which microcracks are generated, can be the "weak" link, since the destruction, as a rule, occurs at the microlevel. Thus, the separation of the total oriented stresses, the identification of the values of the individual components (macro- and microstresses), and the assessment of their contribution make it possible to identify the causes and nature of tool wear and to establish the optimal conditions for their grinding and operation.

Dedication

The authors dedicate this article to the memory of their teacher, Professor M. D. Uzunyan (1934-2020) – the pride of Armenia and Ukraine, a prominent scientist in the field of cutting of materials, researcher and preacher of the diamond spark grinding.

Bibliography

[1] **Tsuge T**. (2009). Radiopacity of conventional, resin-modified glass ionomer, and resin-based luting materials. *J Oral Sci*, **51** 223–230.

[2] **Taguchi K.** et al. (2011). Modeling the performance of a photon counting X-ray detector for CT: energy response and pulse pileup effects. Med. Phys., **38** 81–89.

[3] **Uzunyan, M. D.** (2003). *Diamond-spark grinding of hard alloys*. Kharkov, NTU «KhPI» (In Russian).

[4] **Jadam, T., Datta, S.** (2020). Machinability of Ti-5Al-2.5Sn for electro-discharge machining: an experimental investigation. *Sādhanā* **45,** 238–245.

[5] **Agu, A. C., M. D. Uzunyan, & A. V. Rudnev.** (2018). *Grinding of hard alloys by use of minimum quantity lubrication lechnology* Kharkov, NPU «KhPI» (In Russian).

[6] **Zhao C.** et al. (2006). Study on the active screen plasma nitriding and its nitriding mechanism. *Surface and Coatings Technology*, **201** 231–238.

[7] **Ren D., Liu L.** (2014). Interface microstructure and mechanical properties of arc spot welding Mg-steel dissimilar joint with Cu interlayer, *Mater. Des.* **59** 369–376.

[8] **Zhu D.** et al. (2013). Tool wear characteristics in machining of nickelbased superalloys, Int. J. Mach. Tools Manuf. **64** 60–77.

[9] **Klocke F.** et al. (2011). Influence of temperature on surface integrity for typical machining processes in aero engine manufacture, *Procedia Engineering* **19** 203–208.